Estimating response times, flow velocities and roughness coefficients of Canadian Prairie basins

Kevin R. Shook[1]*, Paul H. Whitfield[2], Christopher Spence[3], John W. Pomeroy[1,2]

[1] Centre for Hydrology, University of Saskatchewan, Saskatoon, SK., Canada

5 [2] Centre for Hydrology, University of Saskatchewan, Canmore, AB., Canada

[3] Environment and Climate Change Canada, Saskatoon, SK., Canada

Correspondence to: Kevin Shook (kevin.shook@usask.ca)

Abstract. The hydrology and hydrography of the Canadian Prairies are complex and difficult to represent in hydrological models. Recent studies suggest that runoff velocities in the Canadian Prairies may be much smaller than are generally

10 assumed.

Times to peak, basin-scale flow velocities and roughnesses were derived from hourly streamflow hydrographs from 23 basins in the central Alberta Prairies. The estimated velocities were much smaller than would be estimated from most commonly used empirical equations suggesting that many existing methods are not suitable for estimating time to peak or lag times in these basins. Basin area was found to be a poor predictor of basin-scale rainfall-runoff flow velocity. Estimated

15 velocities generally increased with basin scale, indicating that slow basin response at small scales could be related to predominance of overland and/or shallow subsurface flow over the very level topography.

Basin-scale Manning's roughness parameters, commonly used in hydrological models, were found to be orders of magnitude greater than values commonly used for streams in other parts of the world. The very large values of roughness call into question whether the Manning equation should be used for modelling runoff on the Prairies. These results have important

20 implications for modelling rainfall-runoff in this region since using widely published values of roughness will result in poor model performance. It is likely that the Darcy-Weisbach equation, which is applicable to all flow regimes, may perform better in hydrological models of this region. Further modelling and field research will be required to determine the physical causes of these very small basin-scale velocities.

1. Introduction

25 Hydrological modelling is notoriously difficult on the Canadian Prairies. The difficulty is due in part to the region's cold climate, the hydrological processes of which which are rarely represented well, if at all, by hydrological models developed for more temperate regions. It is also due to the region's complex hydrography, which is dominated by the presence of millions of depressions which can intercept runoff. Only a few hydrological models are able to simulate the variable contributing areas of Prairie basins which depend on the states of water storage in the depressions (Shook et al., 2013).

30 In addition to the difficulties presented by the region's hydrology and hydrography, recent research has estimated runoff velocities on the Canadian Prairies which appear to be much smaller than are seen in other locations (Costa et al., 2020). If very small runoff velocities are a general feature of the Canadian Prairies, they will also make hydrological modelling difficult, particularly in determining the appropriate values of the roughness parameters required to achieve the required velocities, and therefore flow rates.

35 An example of a very slow Prairie event is shown in Fig. 1, where a flood wave took about 39 hours to travel approximately 1.8 km from the inlet to the outlet of a small (gross area $\approx$ 1.2 km^2) hummocky sub-basin near St. Denis, Saskatchewan, Canada, within the St. Denis Research Basin (SDRB). SDRB is a small (22.1 km^2), relatively hummocky, endorheic basin which has been studied for more than 50 years. The basin is described in detail in Brannen et al. (2015).

The travel time of the flood wave yields a celerity value of approximately 0.013 m s^{-1}. If the flows are entirely overland and
40 turbulent, then Eq. 7 (described below) would imply that the water velocity was less than 0.008 m s^{-1}.

Costa et al. (2020) used a detailed 2D hydrodynamic model (FLUXOS-OVERFLOW) to model flows at Steppler Watershed, a small (~2.1 km^2) basin in southern Manitoba. The only empirical parameter in the model was the vegetation height at which a velocity of zero would occur, which was estimated from the work of Brannen (2015). The model produced overland flow velocities smaller than 0.05 m s^{-1}.

45 Bjerklie (2007) listed bankfull stream velocities between 0.68 and 3.21 m s^{-1} for rivers in Alberta, some of which lie within the Prairies. As the velocities estimated from Brannen et al. (2015) and by Costa et al. (2020) are orders of magnitude smaller than the values of Bjerklie (2007), many questions are raised about a) the causes of the small apparent velocities at St. Denis and Steppler Watershed, b) the extent to which similar values are found in the Prairies, and c) how small velocities can be represented in hydrological models by using appropriate values of roughness coefficients.

Figure 1: Plots of daily rainfall and sub-hourly inflows and outflows for Brannen sub-basin, St. Denis Research Basin, SK, June 13-19, 2013.

50 Slow runoff flows in the Prairies are believed to be influenced by the region's peculiar hydrology and hydrography. The climate of the Prairie ecozone is generally semi-arid, and experiences long, cold winters that freeze soils deeply (Willis et al., 1961; Sharratt et al., 1999). The hydrology of the Prairie ecozone is dominated by cold-region processes, including the accumulation of winter snowpacks (which are controlled by the erosion, transportation, deposition and sublimation of snow by wind), the spring melt of the snowpacks, and infiltration into deeply frozen soils (Pomeroy et al., 1998). Because the soils

55 are generally deep, and the region is semi-arid, soils are rarely saturated (Pennock et al., 2011). Runoff in the region predominantly occurs during the spring melt freshet; runoff due to rainfall events also occurs and may be increasing with changes in precipitation phase and duration caused by climate change (Shook and Pomeroy, 2012; Dumanski et al., 2015). The hydrography of the Canadian Prairies is complex. The typical gentle slopes within the region are partly a product of the continental glaciers that covered the area until comparatively recently (~10,000 years B.P. (Christiansen, 1979)). As the

60 climate is semi-arid, there has not been sufficient energy, time or overland flow to erode conventional drainage systems in much of the region. As shown by Bemrose et al. (2009), the mean annual depths of runoff in Prairie basins are much smaller than in most of the rest of southern Canada. Much of the Prairie precipitation and runoff is trapped in depressions, known

locally as "sloughs" or "potholes". When the depressions are filled, it is possible for flows to occur between depressions, through a process analogous to "fill-and-spill" (Spence and Woo, 2003; Leibowitz and Vining, 2003; McDonnell et al., 2021). Thus, in these basins the areal fraction contributing flows to the outlet is dynamic, changing with the states of water storage in the depressions (Shaw et al., 2012; Stichling and Blackwell, 1957). In Canada those areas that do not contribute flow to a stream or lake for return periods of two years or less because of downstream depression storage are designated "non-effective" (Godwin and Martin, 1975). The extent of the non-effective region within the study region is mapped in Fig. 2.
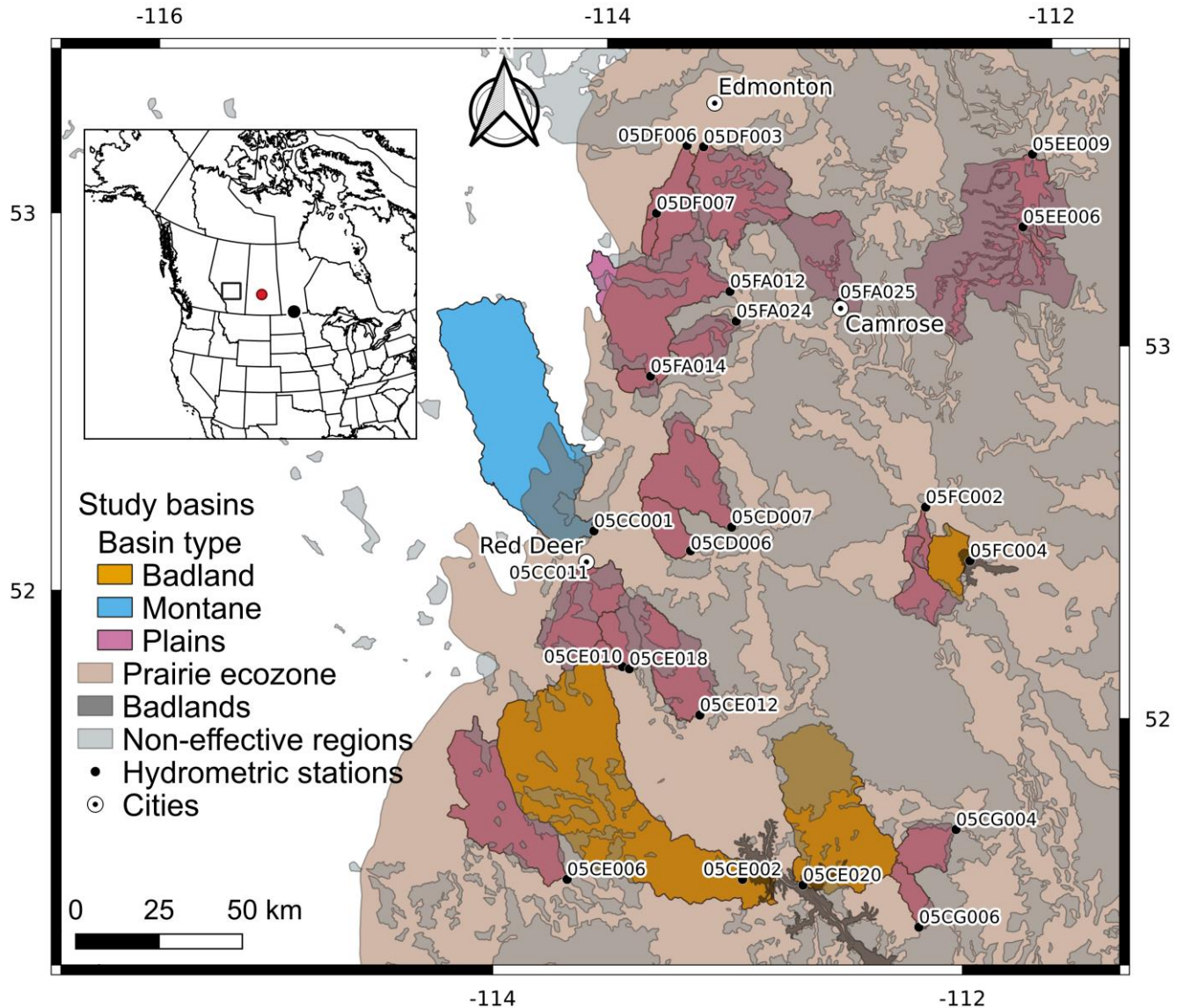
Figure 2: Map of the study basins in central Alberta, shaded by basin type. The Canadian Prairie ecozone (tan shading), non-effective regions (light gray shading) and badlands (dark grey shading) are also plotted. The locations of the gauging stations of

the Alberta study basins are plotted as black dots. The basins are shaded according to their topographic type. Cities within the region are plotted as small dots within circles. The inset map shows the location of the larger map within North America as a rectangle; the locations of SDRB and Steppler Watershed are plotted as a red and black dots, respectively. Projection is UTM13.

70 The objectives of this research are to determine a) if small runoff flow velocities are a general feature of the study area and therefore of the Canadian Prairies, b) if the velocities can be related to any obvious basin-scale parameters, and c) the effects of the flow velocities on basin-scale roughness parameters used in hydrological modelling. This research is intended as a first step in identifying the scope of the phenomenon and will indicate the need for additional detailed field-based research. The results will inform hydrological modelers about the response times of streams in the region and the usefulness of

75 published values of roughness parameters for streamflow modelling on the Canadian Prairies, and will suggest methods for calculating rainfall-runoff velocities that are appropriate for the region.

2. Study area and data

2.1 Study area

The studied region is in central Alberta, Canada, within which there were 23 hydrometric stations gauging unregulated

80 streams during the selected period (2000-2019). This region is under dryland farming, i.e. without irrigation. The locations of the hydrometric stations are shown in Fig. 2. This portion of the Canadian Prairies was selected because it contains a relatively large number of hydrometric stations and a wide variety of topographies and other factors (stream lengths, surface geologies, and depressional storages) believed to influence the basin responses and because it has a good network of precipitation gauges needed to identify high flow events. Alberta's wetland regulations and policies require wetland drainage

85 to be mitigated (Government of Alberta, 2015) and so it is believed that the study region has been less affected by drainage than have been similar regions in Saskatchewan, Manitoba, North Dakota, and Iowa. The centroid of the study region is distant from the previously mentioned SDRB (~480 km) in Saskatchewan and Steppler Watershed (~1090 km) in Manitoba, the locations of which are shown in the inset map in Fig. 2. If small velocities are documented in the study basins, then in concert with the data for Steppler and St. Denis, it may be concluded that they are a feature of the Canadian Prairie

90 landscape.

The basins are dominated by agriculture. According to data sourced from Agriculture and Agri-food Canada (2009), the largest basin fraction classification is annual cropland (mean = 0.49, max = 0.8, min = 0.21) followed by perennial crops and pasture (mean = 0.37, max = 0.65, min = 0.12). The mean developed (i.e., built-up) fraction of the basins is 0.06.

Physical attributes of the selected basins used in empirical equations for basin response times are listed in Table 1. The areas

95 of the selected basins range from 44 to 2,430 km^2. As would be expected in the Canadian Prairies, the basins are relatively level, having main channel slopes ranging between 0.00059 and 0.023 (mean = 0.004). The basin effective fractions (the areas producing runoff with a return period of 2 years divided by the basin gross areas) are between 0.069 (05FA025) and 1

(05CE010 and 05CD006), with a mean value of 0.69 as determined by the Prairie Farm Rehabilitation Administration (Godwin and Martin, 1975).

100 Although all of the hydrometric stations lie within the Prairie ecozone, a small portion of basin 05FA012 lies outside, as does most of the basin of 05CC001, which can be regarded as being largely a montane basin, and which has the greatest basin fraction (0.14) occupied by deciduous trees. Several of the basins (05CE002, 05CE020, and 05FC004) contain badlands, which are deeply eroded river valleys, with exposed clay soils. Basin 05CE020 had the greatest fraction (0.01) of exposed soils. These basins might be expected to respond differently from plains basins in the region, as runoff can be initiated from
105 small rainfall events, and the basins can have subsurface pathways which are very different from other Prairie basins (de Boer and Campbell, 1989). The selected Canadian Prairie basins are classified as being "Plains", "Badland" or "Montane" in plots to determine if there are differences in their responses.

Table 1: Parameters of the study basins in central Alberta.

WSC station	WSC name	Gross drainage area (km²)	Basin effective fraction	Main channel length (km)	Main channel slope (-)	Wetland area (%)	Topographic type
05CC001	BLINDMAN RIVER NEAR BLACKFALDS	1800.0	0.81	125.9	0.0014	6.63	Montane
05CC011	WASKASOO CREEK AT RED DEER	487.0	0.51	51.1	0.0028	3.97	Plains
05CD006	HAYNES CREEK NEAR HAYNES	165.0	1.00	33.1	0.0043	1.91	Plains
05CD007	PARLBY CREEK AT ALIX	511.0	0.88	49.0	0.0006	2.88	Plains
05CE002	KNEEHILLS CREEK NEAR DRUMHELLER	2430.0	0.81	158.5	0.0086	2.72	Badland
05CE006	ROSEBUD RIVER BELOW CARSTAIRS CREEK	753.0	0.85	89.7	0.0012	2.86	Plains
05CE010	RAY CREEK NEAR INNISFAIL	44.4	1.00	13.8	0.0065	3.27	Plains
05CE012	GHOSTPINE CREEK NEAR HUXLEY	506.0	0.62	53.9	0.0039	4.96	Plains
05CE018	THREEHILLS CREEK	199.0	0.69	27.9	0.0035	3.85	Plains

WSC station	WSC name	Gross drainage area (km²)	Basin effective fraction	Main channel length (km)	Main channel slope (-)	Wetland area (%)	Topographic type
05CE020	BELOW RAY CREEK MICHICHI CREEK AT DRUMHELLER	1170.0	0.54	94.0	0.0022	3.13	Badland
05CG004	BULLPOUND CREEK NEAR WATTS	200.0	0.84	31.3	0.0080	3.08	Plains
05CG006	FISH CREEK ABOVE LITTLE FISH LAKE	118.0	0.87	29.5	0.0060	5.50	Plains
05DF003	BLACKMUD CREEK NEAR ELLERSLIE	643.0	0.58	67.6	0.0030	3.49	Plains
05DF006	WHITEMUD CREEK NEAR ELLERSLIE	330.0	0.91	67.8	0.0018	1.96	Plains
05DF007	WEST WHITEMUD CREEK NEAR IRETON	65.4	0.81	17.0	0.0041	2.14	Plains
05EE006	VERMILION RIVER TRIBUTARY NEAR BRUCE	46.4	0.43	27.0	0.0015	9.37	Plains
05EE009	VERMILION RIVER AT VEGREVILLE	1620.0	0.23	128.7	0.0006	7.29	Plains
05FA012	PIPESTONE CREEK NEAR WETASKIWIN	1030.0	0.71	62.3	0.0020	4.42	Plains
05FA014	MASKWA CREEK NO. 1 ABOVE BEARHILLS LAKE	79.1	0.77	22.1	0.0024	3.38	Plains
05FA024	WEILLER CREEK NEAR WETASKIWIN	236.0	0.38	38.8	0.0032	7.30	Plains
05FA025	CAMROSE CREEK NEAR CAMROSE	460.0	0.07	48.7	0.0012	9.02	Plains
05FC002	BIGKNIFE CREEK	281.0	0.69	40.7	0.0228	7.62	Plains

WSC station	WSC name	Gross drainage area (km²)	Basin effective fraction	Main channel length (km)	Main channel slope (-)	Wetland area (%)	Topographic type
05FC004	NEAR GADSBY PAINTEARTH CREEK NEAR HALKIRK	191.0	0.90	37.7	0.0011	8.36	Badland

2.2 Streamflow data

110 The Water Survey of Canada publishes historical daily streamflows. To allow finer determination of basin responses, hourly streamflows for the selected stations were obtained directly from Water Survey of Canada officials. The hourly flows analyzed were restricted to the period May 24 - September 1 in each year, to avoid snowmelt events.

The hourly flows were acquired for the selected stations for the period 2000-2019. This period was selected because it spans both a historic drought (1999-2005) and a recent wet period (2005-2015) experienced in western Canada. Previous research

115 has indicated that the lengths and magnitudes of multiple-day rain events have increased over time in the Canadian Prairies (Shook and Pomeroy, 2012; Dumanski et al., 2015; Szeto et al., 2015). Long-duration rainfall events are more likely than short-duration events to cause basin-wide runoff responses, so a recent period is more likely than an earlier period to contain many basin-scale runoff events. Many of the selected basins responded to large-scale rain events in the summer of 2011 (not shown here).

120 Manual gauging data (velocities and cross-sectional areas) were obtained directly from Water Survey of Canada for the study stations, for the period 2010-2015. As is described below, the values were used to create open-water rating curves to estimate flow velocities from stage values.

2.3 Rainfall data

Daily rainfall values were downloaded from the Environment and Climate Change Canada website

125 (https://climate.weather.gc.ca/) using the **R** (R Core Team, 2013) package **weathercan** (LaZerte and Albers, 2018) for every available station within the study basins during the study period. Basin mean daily rainfalls were determined for each event analysed by gridding the station data using the **R** package **gstat** (Pebesma, 2004), using inverse-distance weighting, clipping the resulting grid to the basin boundaries using the R package **raster** (Hijmans, 2020) and calculating the mean of all grid cell values within the basin. The intent in determining the mean daily rainfalls was only to confirm the existence of rainfall

130 events which occurred before the streamflow peaks. Daily rainfall values were sufficient for this purpose.

2.4 Basin topographic data

Shapefiles of the selected hydrological basins were obtained from Environment and Climate Change Canada. Digital Elevation Models (DEMs) were obtained from the Shuttle Radar Topography Mission (SRTM) (Farr et al., 2007), SRTM version 3.0 (Siemonsma, 2015). The SRTM data have a vertical precision of 1 m and a horizontal resolution of 1 arc-second
135 (approximately 30 m). The DEMs were used to delineate the basin channels, and to estimate slopes for the study basins. All slopes presented herein are dimensionless (i.e. m/m). Basin hypsometric curves, (plotted in Fig. 3), demonstrate that two of the Badland basins (05CE002, and 05CE020) and the Montane basin (05CC001) have more relief than any of the Plains basins.
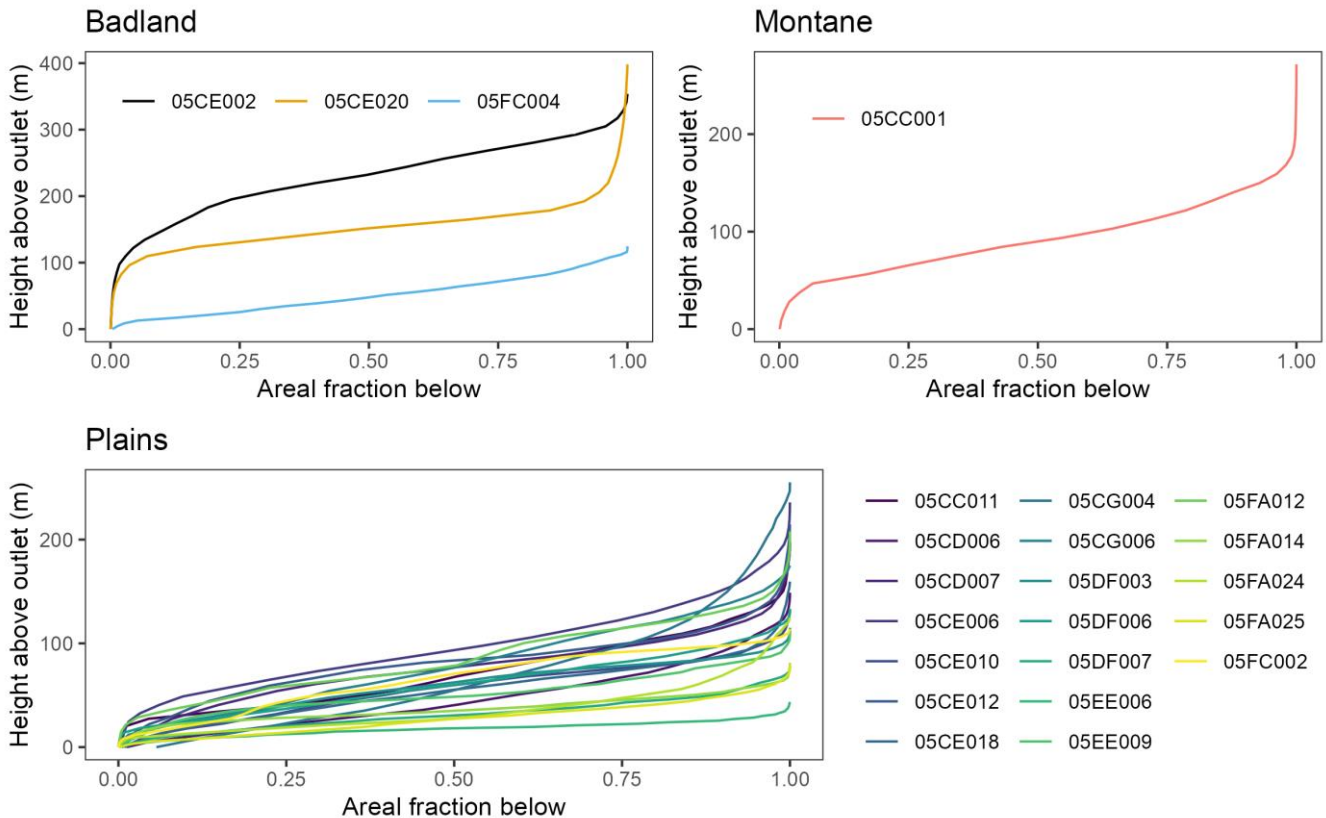
Figure 3: Hypsometric plots of study basins, by basin topographic type.

3. Methods

140 As snowmelt runoff events dominate the hydrology of the Canadian Prairies, it might be assumed that snowmelt events would be the most useful to analyse the responses of prairie basins. Snowpacks are spatially extensive, thereby ensuring that most or all of a basin is responding to a given event. However, snowmelt-runoff events are much more complex than rainfall

events. Within the Canadian Prairies, the ratios of instantaneous peak flows to daily peak flows have been shown to differ between rainfall and snowmelt events (Ellis and Gray, 1966). The spring melt of a prairie snowpack is a slow process,

145 generally taking many days, and is controlled by the diurnal fluctuations of air temperature and, especially, incoming solar radiation (Pomeroy et al., 1998). As snow melts, the meltwater must travel through the snowpack via matrix flow and preferential paths (Leroux and Pomeroy, 2017), the lengths of which will change as the pack melts. Snow redistribution by wind causes highly variable snowpacks and extended snowcover depletion periods of partial snowcover and therefore partial contributing area for runoff (Shook and Gray, 1997). Runoff can be impeded by deep, cold snow drifts because of the

150 transport of snow by wind (Pomeroy et al., 1993) further slowing the translation of runoff to streamflow (Woo and Sauriol, 1980).

Compared to those generated by snowmelt, rainfall-runoff events are simpler. Flow velocities estimated from rainfall events can provide base estimates of basin responses. As is described in the next section, there are many existing empirical equations for basin response times. It is useful to compare the response times of Prairie basins to these empirical

155 relationships to determine if Prairie basins are slower to respond than would be expected from existing equations. All of the empirical equations are, however, based on rainfall events, meaning that only values derived from rainfall can be compared. For all these reasons, only rainfall-runoff events are evaluated here.

The research objectives were answered by a) estimating the observed response times of the 23 experimental basins to rainfall-runoff, b) determining the expected response times from existing empirical equations, c) estimating the observed

160 flood wave celerities and basin-scale velocities, and d) determining basin roughness factors.

The premise of this research is that the hydrological responses to rainfall and underlying runoff velocities in Prairie basins are much slower than in many other regions. To avoid false confirmation of the premise, all assumptions herein are made to be as conservative as is possible, i.e. acting to maximize the estimated basin velocities.

3.1 Observed basin response times

165 There are many ways of quantifying observed response times of basin streamflows to rainfall-runoff, including the time of concentration (t_c), lag time (t_l), and the time to peak (t_p). These terms have been present in the hydrological literature for a long time, although the distinctions amongst them are rarely clear (Gericke and Smithers, 2014), and the terms may have multiple definitions (McCuen, 2009). Gericke and Smithers (2014) demonstrated four different definitions of t_c, two of which have also been used to define t_l. They also demonstrated conflicting definitions between t_p and t_l. The meanings of

170 time of concentration (t_c), lag time (t_l), and time to peak (t_p) are defined here as follows.

Lag time (t_l) is defined as the time between the centroid of effective rainfall, i.e. that exceeding a loss function, and that of the peak discharge (Gericke and Smithers, 2014). Determination of t_l requires modelling rainfall losses.

Time of concentration (t_c) as a concept dates from at least 1851 (Beven, 2020) and is considered to be the time required for water to travel from the most distant point in the basin to the outlet. There is no way to ascertain this value experimentally

175 (Langridge et al., 2020).

Time to peak (t$_p$), was defined by Gericke and Smithers (2014) as "the time from the start of effective rainfall to the peak discharge in a single-peaked hydrograph", i.e. from the onset of runoff to the peak. However, the methodology applied here uses the more recent definition of Langridge et al. (2020), which is "the rise time of a storm hydrograph, encompassing the time from the first stream contributions from a precipitation event to the arrival of the peak flow". Using this definition, it is relatively straightforward to determine the value of t$_p$ directly from event hydrographs.

3.2 Observed time to peak

Times to peak were estimated for the selected basins from observed event hydrographs, similar to the procedures of Holtan and Overton (1963) for estimating basin response times. The procedure consisted of a) identifying peak flows, b) selecting events with simple peaks, and c) determining the time of the initial point of rise for each event, and d) subtracting time of the initial rise from that of the peak flow. An example of a typical peak event, for basin 05CC001, is shown in Fig. 4.

Peaks were identified in the hourly WSC flows, for summer (May 24-Sept 1) periods, using a variant of the function ch_get_peaks in the **R** package **CSHShydRology** (Anderson et al., 2019). The modification was necessary to adapt the function to work with hourly, rather than daily flows. The function extracts peaks over a threshold, here the 80th quantile was used. The function extracts sequences of points greater than the threshold and prepends and appends values for four additional time steps to ensure a time series of at least nine values where only a single hour exceeds the threshold. In total, 195 peaks were identified among the basins.

A subset of 101 simple events was extracted; these events had low flows before the event, several days of rainfall, and an obvious single peak. The identification of simple peak events is potentially arbitrary but was conservative as the process could only reduce the maximum values of t$_p$ estimated for the basins. The initial point of rise for each event was defined as being the time when the flows exceeded 1% of the difference between the minimum flow and the peak flow. This threshold was used to avoid any effects of small variations in hourly streamflows.
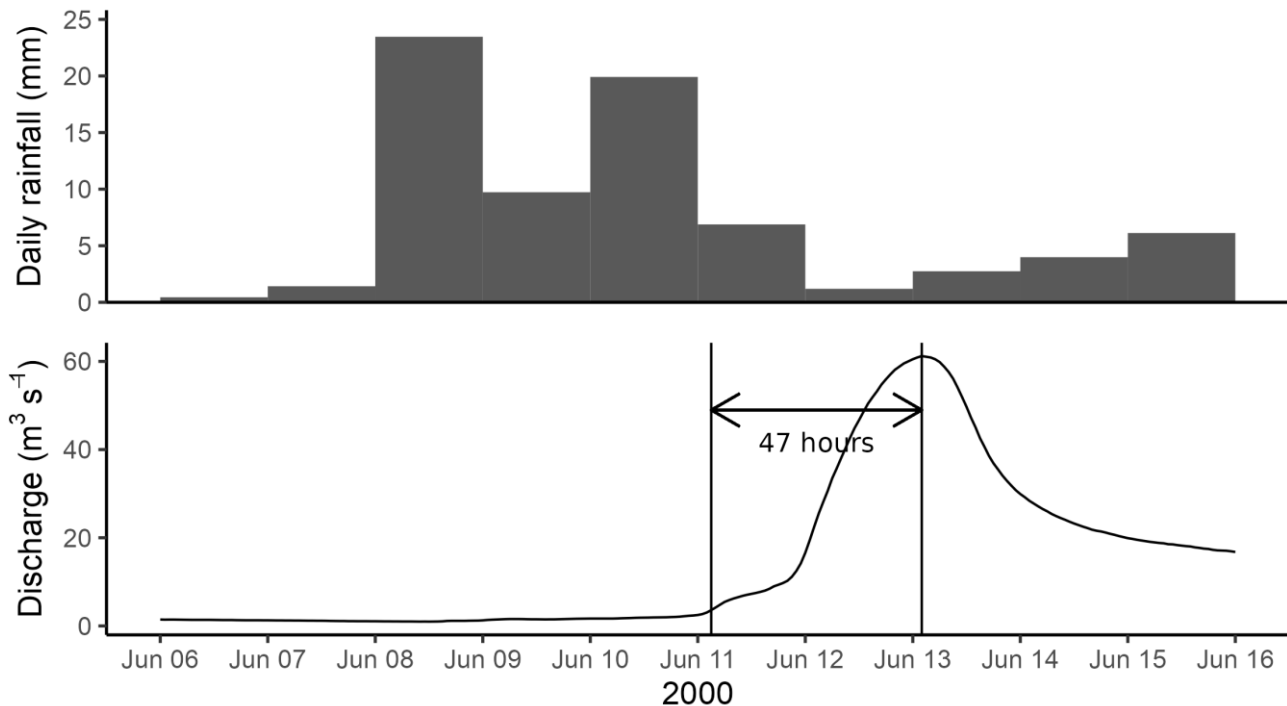
Figure 4: Mean basin daily rainfall and hourly discharge hydrograph of station 05CC001, BLINDMAN RIVER NEAR BLACKFALDS. The peak occurs on June 13 at 02:00. The period of rise begins at 03:00 on June 11, resulting in a time to peak of 47 hours.

Many of the basins are large (maximum gross area = 2430 km²) and it is difficult for rainfall events, particularly for intense convective storms, to cause basin-wide responses. The largest event time to peak for each basin was selected as the value of the basin t_p, as it is assumed to best represent the response of the basin. It is possible that the actual t_p of a basin may exceed that of the longest event in our time series. Precipitation events large enough to cause runoff over a whole basin may have durations of runoff smaller than the time of concentration of the basin, causing the basin responses to be asynchronous, and resulting in reduced peak times. Thus, the maximum observed peak time may underestimate the true response time of a basin. So the assumption that the entire basin is contributing flow to the events is conservative.

3.3 Response times from existing empirical equations

Published empirical equations were used to estimate the values of t_l, t_p and t_c for the study basins. As noted by Grimaldi et al. (2012), the values of t_c (and therefore consequent estimations of flow velocities and roughness parameters) computed using empirical relationships can vary widely, up to 500% in their study, for a given basin. Therefore several empirical equations were used to estimate the response times of the study basins.

Modelling based on these empirical relationships requires caution and understanding of the assumptions of any chosen for use. The empirical relationships are based on quite limited sets for observations and extrapolation to different landscapes can be challenging. As will be seen, most available empirical equations fail on the landscapes in this study so modelling based on those relationships is likely to be unsuccessful.

The definitions of these response times are similar enough that they can be compared with the observed t_p values, despite the differences described above. Note that the equations given below are as they are taken from the literature, so the symbols used, and their units, vary. The values of the basin parameters used by the empirical equations are given in Table 1. Each of the empirical response times is denoted by a letter designating the researcher whose whose equation is used. For example, t_c as developed by Kirpich (1940) is designated as t_{cK}. The designation is applied to the equation and to values calculated from the equation of each researcher.

Sheridan (1994) and Gericke and Smithers (2014) list many equations for estimating response times of rainfall-runoff hydrographs in flat regions. The equations used in this study to estimate basin response times were selected because they employ simple parameters based on basin dimensions (such as the area, and the length and slope of the main stream channel), without requiring regionally specific coefficients that may not be available for the Canadian Prairies. The equations were also selected to avoid parameters, such as stream density, which are difficult to apply to intermittent streams such as those in Prairie basins or would be unavailable.

The equation of Kirpich (1940) for t_c was developed for very small (areas between 0.005 and 0.453 km^2), and comparatively steep (slopes between 0.0399 and 0.0978) basins in Tennessee. Kirpich (1940) stated that the relationships used to derive the equation were valid "for the average small agricultural area ranging from 1 to 200 acres" i.e., between 0.004 and 0.81 km^2. Despite its unsuitability for Prairie basins, the equation is included here because it familiar to many hydrologists. The equation (as cited by Gericke and Smithers (2014)), defines the time of concentration, t_{cK} (hours), based on the main channel length (L_c, km) and the main channel slope (S_c) as

$$t_{cK} = 0.0663\left(L_c{}^2/S_c\right)^{0.385}. \qquad (1)$$

Although stream channel delineations are available from Natural Resources Canada (2004), the stream channel vectors are discontinuous in many places, probably because of the effects of depressions. Therefore, the main channel length was calculated from the SRTM DEM of each basin, using the Free Open Source Software (FOSS) GIS **WhiteboxGAT** (Lindsay, 2016). The value of S_c was calculated as the difference in elevation between divide and outlet (m), divided by L_c converted to m.

Watt and Chow (1985) developed a relationship for t_l (in hours) as

$$t_{lW} = 0.000326\left(L_c/\sqrt{S_c}\right)^{0.79}. \qquad (2)$$

The equation was developed for basins in the midwest United States and Quebec having areas between 0.005 and 5,840 km^2, channel slopes between 0.001 and 0.09 and main channel lengths between 100 m and 200 km (Watt and Chow, 1985), so it can be considered to be applicable to the study basins (see the basin parameters in Table 1).

James et al. (1987) developed t_p equations from 48 basins having areas between 0.73 and 62.2 km^2 in Arizona, Arkansas, Iowa, Louisiana, Mississippi, Nebraska, North Carolina, Ohio, Oklahoma, Tennessee, Texas, Virginia, and Wisconsin. James et al. (1987) defined t_p as "the time from the beginning of the rainfall excess to the peak discharge (hr)", which is the same definition as that of Gericke and Smithers (2014).

The equation for the flattest basins (i.e. where slope < 5%), is a function of A, the basin area (km^2), HT, the maximum difference in elevation between divide and outlet (m), and L the distance to the divide (km):

$$t_{pJ} = 0.97 A^{0.4} HT^{-0.2} L^{0.2}. \qquad (3)$$

The distance to the divide (L) is defined here as the Euclidean distance from the outlet to the farthest point on the basin divide. For the study basins, the location of the farthest point from the outlet was determined by clipping the SRTM DEM using the shapefile of the basin divide and finding the distance from each DEM cell on the raster divide to the outlet, with an **R** script using the packages **raster** (Hijmans, 2020) and **sp** (Pebesma and Bivand, 2005). The value of HT was estimated by the same script as the difference in elevation between the highest cell on the basin divide, and that of the outlet.

Capece et al. (1988), related t_l (hours) to the drainage area (A, ha) and also included the percentage of wetlands (W) as

$$t_{lC} = 3.0 + 0.38 (A^{0.11})(W + 1)^{0.71}. \qquad (4)$$

The Florida basins modelled in Capece et al. (1988) were very small (areas between 0.08 and 14.5 km^2). The basin slopes ranged between 0.0008 and 0.0015. The "percentage of wetlands" varied between 0 and 23, however the meaning of this term is uncertain. It is believed to refer to the percentage of the wetland area within each basin.

W was calculated for each of the basins in this study, by obtaining wetland percentages for homogeneous polygons from Alberta Agriculture and Forestry, Government of Alberta (2016). The polygons were weighted by their areas, clipped to the experimental basin boundaries, and then aggregated, using the FOSS GIS program **QGIS** (QGIS Development Team, 2009). The values of W for the experimental basins ranged from 1.9% to 9.4%.

Sheridan (1994) compared several empirical equations, including those of Capece et al. (1988), James et al. (1987), Kirpich (1940), and Watt and Chow (1985), to experimental values for nine flat basins in the south-eastern United States, finding that all the empirical equations studied grossly underestimated the actual responses. In response, Sheridan (1994) developed a simple empirical equation for t_c (hours) based on the basin drainage area (DA, km^2):

$$t_{cS} = 2.96 \, DA^{0.54}. \qquad (5)$$

The basins used by Sheridan (1994) were small, having areas ranging from 2.62 to 334 km^2. The channel slopes ranged between 0.001 and 0.0035.

Langridge et al. (2021) developed a modified version of the model first presented in Langridge et al. (2020). The revised model replaced coefficients defining the basin wetness, which required values rarely measured in North America, with coefficients whose values are more easily determined. The revised Eq. 6 for t_p (hours), is based on Q_p (peak stream flow (m^3 s^{-1}), and L, the longest drainage path (km):

$$t_{pL} = \left(\left(C_1 \frac{L}{\sqrt{S}} \right) + \left(C_2 \frac{Q_p}{DA} \right)^{-\frac{1}{3}} \right)^2. \quad (6)$$

The exact meaning of the definition of L is unclear, so it is assumed that the value of L is the same as that of L_c in Eq. 3. The values of C_1 and C_2 (dimensionless) are taken from 9 classifications, determined by the historical wetness of the basin and the season. The historical wetness of the basin is indexed by R_c, the ratio of mean annual discharge depth to mean annual precipitation. According to Langridge et al. (2021), "wet" basins have R_c values greater than or equal to 0.7; basins having R_c values less than 0.5 are classified as "dry". Values of C_1 and C_2 are provided for "wet", "average" and "dry" basins in seasons which are assumed to be "Wet" (December through March), "Dry" (June through September) and "Average" (April, May, October, and November). The modified model was tested for basins in the UK, Massachusetts, and Ontario.

Values of R_c computed from historical precipitation and streamflows for the experimental basins were found to be between 0.019 and 0.068, the mean being 0.041. These are typical of values found in the western Canadian Prairies. The corresponding values of C_1 and C_2 for dry basins during the dry season, as determined from the plot in Langridge et al. (2021), were 0.0031 and 0.9593, respectively.

None of the empirical equations was developed from basins exactly like those in this study. The areas of the basins used to develop the equation of Watt and Chow (1985) overlap those of the selected central Alberta basins and the channel slopes are similar, but the equation "has not been tested and may not apply for … basins with large lake and swamp storage". The large depressional storages of many of the experimental basins indicate that the equation may not apply to them.

The equation of James et al. (1987) was developed for fairly level basins, but their range of areas only overlaps the 5 smallest study basins presented here. The equation of Capece et al. (1988) was developed for very flat basins containing wetlands, but the basins used for developing the equation were smaller than any basin selected for this study. The areas of the basins used by Sheridan (1994) overlap those of the study basins, but the original basin areas in ponds and lakes ranged between 0.11 and 2.34%, which are much smaller than in many Prairie basins. The areas of the basins used by Langridge et al. (2021) are not known, but the climates of their basins are far wetter than the Canadian Prairies.

3.4 Wave celerities and water velocities

For each basin, the celerity of the flood wave (McDonnell and Beven, 2014) was calculated by dividing the observed value of L_c by t_p. The actual distance that water flows in each event is unknown, particularly for those basins which have large non-effective fractions, where the area of the basin contributing flow is strongly influenced by the storage of water in depressions. However, the use of L_c derived from the gross drainage area is conservative, as it represents the maximum distance that water could travel; dividing L_c by t_p can only overestimate the celerity of an event.

The relationship between the celerity of a wave (c) and the water velocity (v) is often expressed as

$$c = \beta v, \quad (7)$$

where β is a constant.

305   Many theoretical relationships have been developed for β, depending on the channel properties (dimensions, roughness), but a value of 5/3 is often used for wide channels with turbulent flows (Wong and Zhou, 2006). As velocities decrease, the value of β increases. When flows are fully laminar, $\beta = 3$ (Wong and Zhou, 2006). Therefore, when flows are turbulent, basin scale water velocities can be estimated from flood wave celerities by solving Eq. 7 for v, assuming that $\beta = 5/3$. As is discussed below, the regime(s) of the flows in this study are unknown and may lie in the laminar region, in the transition

310   from turbulent to laminar flow, or be fully turbulent as Reynolds numbers for shallow overland flow are not necessarily in the turbulent range (Schroers et al., 2022). Estimating the velocities from the celerities by assuming $\beta = 5/3$ is conservative for this study in that it gives larger estimated velocity values.

Observed streamflow velocities provide useful comparisons with the empirically derived and computed basin-scale flood wave velocities. As velocity data are not generally available at the time of peak flows, stream velocities were estimated from

315   manual depth-velocity streamflow measurements taken at the hydrometric stations. These values were supplied by Water Survey of Canada staff. The mean velocity of a stream is a power-law function of the hydraulic radius (Eq. 9), which approximates the depth of flow in a natural channel. Rating curves relating the discharge of a stream to its stage are also typically power-law functions. Therefore, the relationship between the mean velocity and the discharge at a point is assumed to also be a simple power-law. Curves of the mean stream velocity as a function of discharge were developed by fitting

320   linear models of the $\log_{10}$ values of the observed mean velocities vs the $\log_{10}$ values of the observed discharges. The velocity-discharge curve from each gauging site was used to estimate stream velocities from the peak flows corresponding to the t_p values.

Manual gauging values obtained between May 24 and September 1 (which very conservatively approximate the frost-free period in the Canadian Prairies) were used to develop the rating curves, to ensure that the values were not affected by ice. A

325   threshold of at least five manual gauging values through the study period was selected as the minimum needed to derive a curve. Because the water depths and velocities were zero during many of the summer manual gaugings, curves could only be derived for 18 streams.

3.5 Basin roughness coefficients

Roughness coefficients were estimated from basin-scale flow velocities calculated from the observed t_p values and the basin

330   dimension parameters. The roughness coefficients can be compared to other study values to evaluate the suitability of commonly used equations for modelling streamflows in these basins.

3.5.1 Manning's n

The Manning open-channel flow equation is widely used in hydrology, although its usefulness has been questioned (Ferguson, 2010). In Europe, Manning's equation is known as the Gauckler–Manning–Strickler or the Gauckler–Manning

335   formula. Manning's equation is expressed in SI units as (Schneider and Arcement, 1989) as a function of v (stream velocity,

m s^{-1}), R (hydraulic radius, m), S_e (slope of the energy grade line (dimensionless) which is approximated by the stream slope S), and n (roughness coefficient, m$^{-1/3}$ s):

$$v = \frac{R^{\frac{2}{3}}S_e^{\frac{1}{2}}}{n}. \qquad (8)$$

To test the applicability of Manning's equation to the region of interest, Eq. 8 is solved for n, using experimentally derived
340 values for v, R and S. The values of n produced in this manner are basin-scale estimates and are *not* intended to be used for modelling or other calculations.

The hydraulic radius is defined as the quotient of a (cross-sectional area of flow, m^2), and w_p (wetted perimeter, m):

$$R = \frac{a}{w_p}. \qquad (9)$$

As Q = v a, a = Q / v, where the value of Q is that of the peak discharge for each of the events.
345 Assuming rectangular cross-sections of flow, the flow width (w) and depth (d) are related to a as

$$a = wd = d^2\frac{w}{d}, \qquad (10)$$

so knowing a, and assuming a value of w:d, the depth can be estimated. Similarly, the wetted perimeter can be estimated as

$$w_p = w + 2d = d\frac{w}{d} + 2d. \qquad (11)$$

For gently sloping rivers in Canada, the US and New Zealand (i.e. having slopes less than 0.005), width:depth ratios have
350 been found to be as great as 40 (Rosgen, 1994). Bjerklie (2007) listed bankfull width:depth ratios for 19 Alberta rivers, with values ranging from 11.1 to 66, with a mean of 37.9. Using the manual gauging values, the mean depth can be estimated as the quotient of the cross-sectional area and width of flow. The maximum width:depth ratio was selected for each station to estimate Manning's n as it is most conservative; small values of w:d will result in large values of n. The maximum width:depth ratios were determined for all gauging sites (min = 13.2, mean = 48.2, max = 144) and values of n were
355 estimated for all basins.

3.5.2 Darcy-Weisbach f

The Darcy-Weisbach equation, although less widely used than Manning's, has the advantage of being applicable across all flow regimes, from laminar to fully turbulent. Darcy-Weisbach roughness coefficient f values (dimensionless) were calculated from the study velocities. Comparing the study f values to published empirical values derived from research plots
360 allows determination of the ability of the Darcy-Weisbach equation to be used as a robust routing method in hydrological models in gently sloping agricultural basins.

For open-channel flows, the equation for f can be written as (Gilley et al., 1992), where g is the acceleration of gravity (9.81 m s^{-2}):

$$f = \frac{8gRS}{v^2}. \qquad (12)$$

4. Results

4.1 Observed times to peak

In total, 101 clear, simple rainfall-runoff events were found among the 23 basins. Hydrographs demonstrate that the observed times to peak varied widely amongst, and within, basins (Fig. 5). In the majority of the basins (05CC001, 05CD006, 05CD007, 05CE002, 05CE012, 05CE018, 05CE020, 05CG006, 05DF003, 05DF006, 05DF007, 05FA024, 05FC002), the largest events in each basin have similar response times (Fig. 5). Several basins (05CC011, 05EE006, and 05FA024) display flashy event hydrographs showing sharp rising and falling limbs, with short times to peak. It is assumed that these events were caused by runoff events that did not cause much of the basin to respond. Although the hydrographs are coloured according to the basin topographic type, there does not seem to be substantial differences in the responses by basin type. Basin 05FA025 had only a single event, which featured a slow rise, followed by a flat response and a delayed peak. The shape of the hydrograph was due to the basin's very slow responses to two precipitation events. To avoid over-estimating the basin response time, the "shoulder" of the hydrograph, which was the response to the first event, was taken as the peak, resulting in a time to peak of 190 hours.
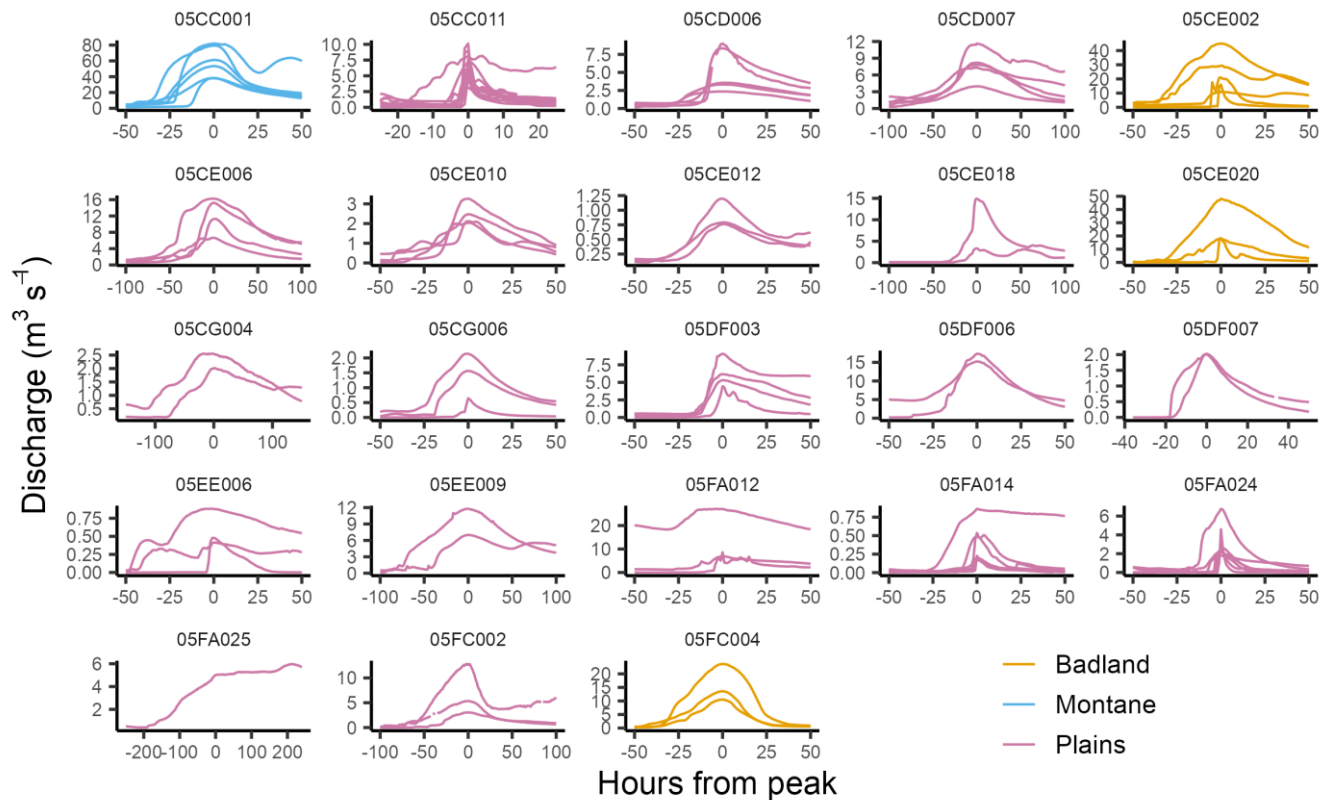
Figure 5: Hydrographs of all events by basin, coloured according to basin topographic type. Note that the scales of the axes vary

among the panels.

The observed event times to peak are provided in the published data set. Table 3 lists the observed t_p value (i.e. the maximum event t_p) for each basin. There appears to be little relationship between observed t_p and the basin parameters as shown by the

380 correlation coefficients of linear models in Table 2. The lack of any significant correlation with the gross basin area is particularly surprising, given that the empirical equations of James et al. (1987), Capece et al. (1988) and Sheridan (1994) are functions of the basin area, and those of Kirpich (1940) and Watt and Chow (1985) are functions of L_c, which is a function of basin area (Gray, 1961).

Table 2: Values of the correlation coefficient (R²) and slope for linear models of the observed t_p vs. basin variables.

Variable	R²	slope
Gross area	0.0001	-0.001
Effective area	0.0065	-0.008
Effective fraction	0.0350	-35.356
$S^{0.5}$	0.0156	-191.555
Wetland area percent	0.0171	2.518
Qp	0.0057	-0.295

385 ## 4.2 Empirical equation response times

Fig. 6 plots the empirical equation response times against the observed t_p for each study basin. The empirical t_l, t_c, and t_p values computed from the Capece et al. (1988) (mean ratio of empirical:observed = 0.226), James et al. (1987) (mean empirical:observed ratio = 0.219), Kirpich (1940) (mean empirical:observed ratio = 0.165), and Watt and Chow (1985) (mean empirical:observed ratio = 0.214) equations are much smaller than the corresponding observed t_p for each basin. The

390 basin topographic type did not influence the values of t_{lC}, t_{pJ}, t_{cK} or t_{lW}.

The values of t_{cS} (mean empirical:observed ratio = 1.184) and t_{pL} (mean empirical:observed ratio = 1.683) were much more similar in magnitude to observed t_p than were the other empirical values. The good agreement between t_{cS} and t_p is not surprising as the equation was specifically developed for slow-responding basins. The relatively good agreement between t_{pL} and the observed t_p values is interesting because many of the equation parameters (L, S, DA) are also used by the other

395 empirical equations which fared much worse. It is worth noting that unlike the other equations, Langridge et al. (2021) includes the effects of climate (though the constants C_1 and C_2) and the peak discharge.
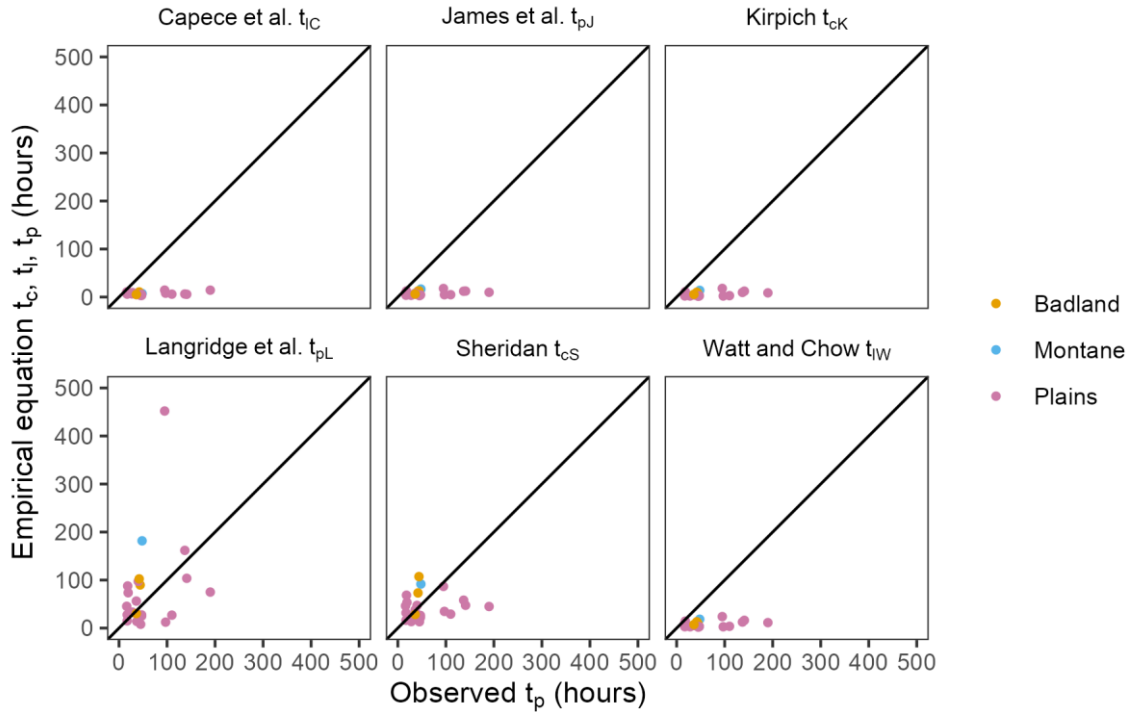
Figure 6: Empirical equation t_l, t_c and t_p vs. observed t_p for the study basins. The points are coloured according to the basin topographic type. The lines are 1:1.

4.3 Observed basin flood wave celerities and velocities

The observed celerities, (Table 3), are as small as 0.071 m s⁻¹. The calculated water velocities range from 0.043 to 0.6 m s⁻¹ (mean = 0.24 m s⁻¹). It is important to note that these values are basin-scale averages; they do not represent the velocity of

400   flow at the outlet, or at any other point.

As discussed above, there was no significant relationship between observed t_p and basin area. It is known that the magnitude of L_c generally increases as a power function of basin area (Gray, 1961). Therefore, the velocity would be expected to show a positive trend with basin area, as is shown in Fig. 7, but the relationship is weak (R^2 = 0.37). The Badland and Montane basins show very little deviation in their relationship between basin velocity and area; therefore, it is likely that their

405   behaviour is primarily differentiated from the Plains basins by their relatively large basin areas.

Table 3: Observed basin t_p, calculated flood wave celerity, basin velocity, Manning n, and Darcy-Weisbach roughness f, for the study basins.

WSC station	Observed t_p (h)	celerity (m s⁻¹)	velocity (m s⁻¹)	n (m⁻¹ᐟ³/s)	f (-)
05CC001	48	0.73	0.44	0.12	0.72
05CC011	16	0.89	0.53	0.08	0.39

WSC station	Observed t_p (h)	celerity (m s^{-1})	velocity (m s^{-1})	n (m$^{-1/3}$/s)	f (-)
05CD006	47	0.20	0.12	0.70	26.64
05CD007	141	0.10	0.06	0.58	19.25
05CE002	44	1.00	0.60	0.16	1.34
05CE006	137	0.18	0.11	0.42	8.68
05CE010	45	0.09	0.05	1.75	192.21
05CE012	40	0.37	0.22	0.13	1.64
05CE018	37	0.21	0.13	1.09	52.38
05CE020	42	0.62	0.37	0.15	1.01
05CG004	110	0.08	0.05	1.67	170.60
05CG006	47	0.17	0.10	0.60	25.58
05DF003	19	0.99	0.59	0.08	0.36
05DF006	36	0.52	0.31	0.24	2.53
05DF007	17	0.28	0.17	0.32	8.33
05EE006	28	0.27	0.16	0.20	2.61
05EE009	95	0.38	0.23	0.17	1.05
05FA012	18	0.96	0.58	0.05	0.21
05FA014	27	0.23	0.14	0.27	3.88
05FA024	17	0.63	0.38	0.16	1.42
05FA025	190	0.07	0.04	1.90	148.44
05FC002	97	0.12	0.07	4.78	1232.36
05FC004	36	0.29	0.17	0.51	5.99
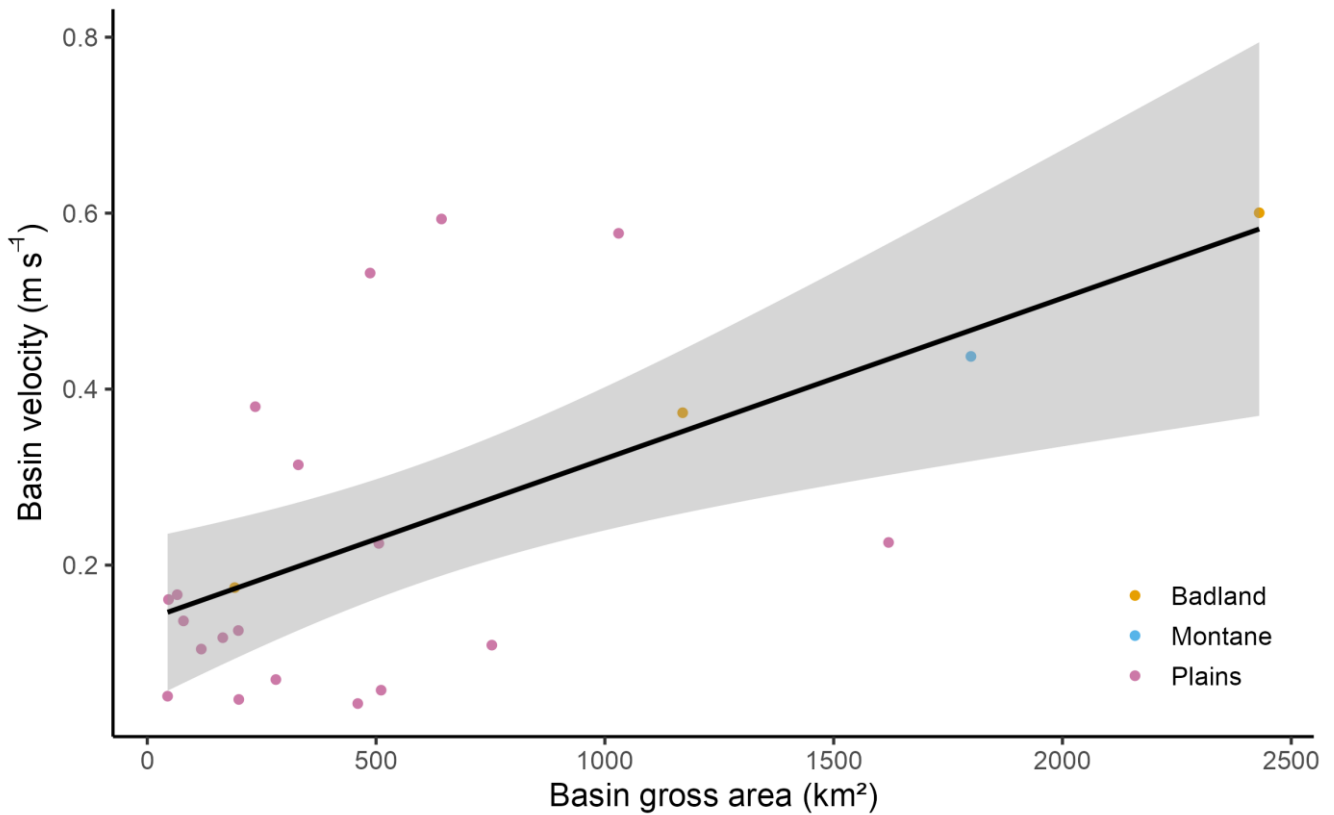
Figure 7: Basin velocity vs. gross area of each basin. The line represents a least-squares linear model. The gray region is the 95% confidence interval of the regression ($R^2 = 0.37$).

The ratios of basin velocities to the stream velocities show an increasing trend ($R^2 = 0.24$) with basin area (Fig. 8). The basin velocities varied from 0.03 to 0.65 (mean = 0.3) of the estimated stream velocities. As with the plot of basin velocities, the velocity ratios of the Badland and Montane basins were like the values for Plains basins of similar areas. As all the velocity ratios were smaller than 1, it appears that the methodology for estimating the stream velocities is not grossly in error.
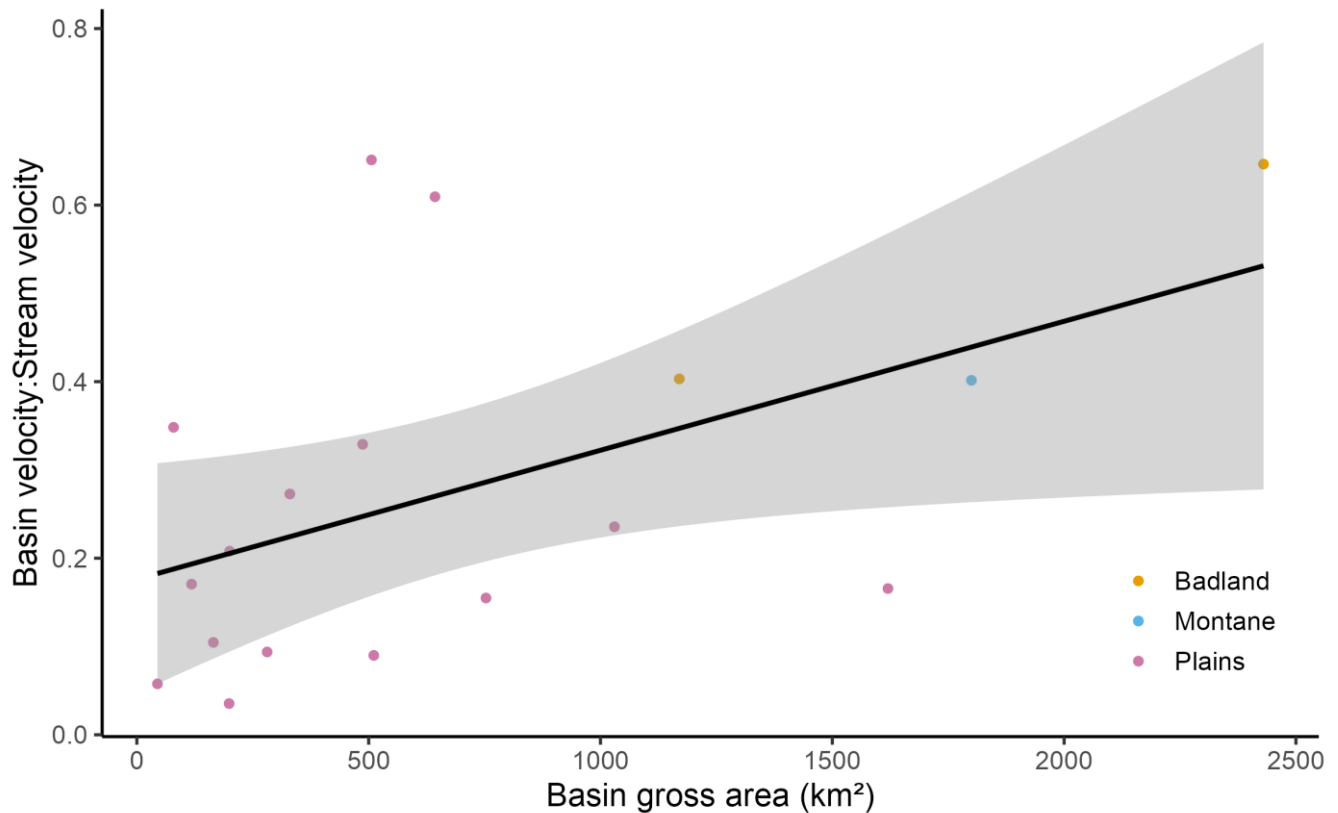
Figure 8: Ratio of basin velocity to stream velocity vs. gross area of each basin. The line represents a least-squares linear model. The gray region is the 95% confidence interval of the regression ($R^2 = 0.24$).

4.4 Observed basin roughness coefficients

4.4.1 Manning's *n*

415 The magnitudes of *n*, as plotted in Fig. 9, varied widely (min = 0.053, mean = 0.7, max = 4.8). As a reference, the maximum *n* value given by Schneider and Arcement (1989) is 0.3, for flows through a forested floodplain, and Weltz et al. (1992) found values of *n* as large as 0.56 for small (3.05 m x 10.7 m) plots on prairie grasslands in the US. The large values of *n* calculated here imply that Manning's equation does not adequately describe the flows in many of the small basins, as the values are far too large to be plausible. The values of *n* for basins having gross areas greater than 1000 km² are consistently

420 relatively small, as shown by their proximity to the dashed line in which represents the base *n* value for a straight stable channel, as suggested by Schneider and Arcement (1989). As with the plot of basin velocity (Fig. 7), the Badland and Montane basins behave similarly to the Plains basins having similar areas.
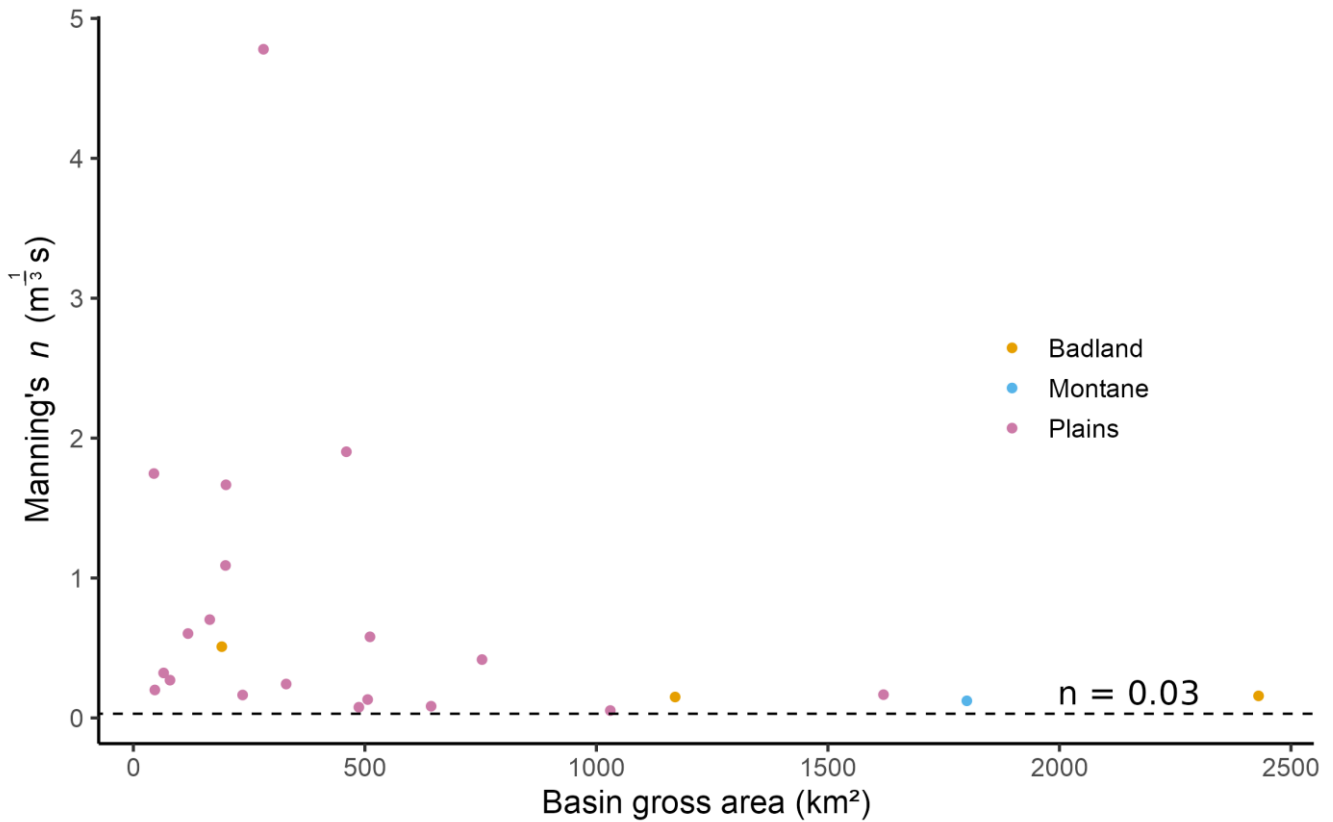
Figure 9: Manning's *n* vs. gross area of each basin. The dashed horizontal line represents the value of *n* for a clear straight channel (0.03).

4.4.2 Darcy-Weisbach roughness coefficient *f*

The calculated values of *f*, listed in Table 3, varied over more than four orders of magnitude (min = 0.21, mean = 83, max =
425   1232). The values of *f* for basins 05FA025, 05CG004, 05CE010, 05CD007, 05CE006, 05FA014, and 05EE006, plot within,
or adjacent to, the values of Bond et al. (2020b) (as listed in Bond et al. (2020a)) , and Abrahams et al. (1994) in Fig. 10. The
agreement between the observed points and the published values is remarkable considering a) that the published values were
all derived from very small experimental plots, rather than from basin-scale observations and b) the many assumptions which
went into the derivation of the observed values.
430   As listed in Table 3, the Manning's *n* values computed for these basins were 1.90, 1.67, 1.75, 0.58, 0.42, 0.27, and 0.20,
respectively, which are too large to be plausible.
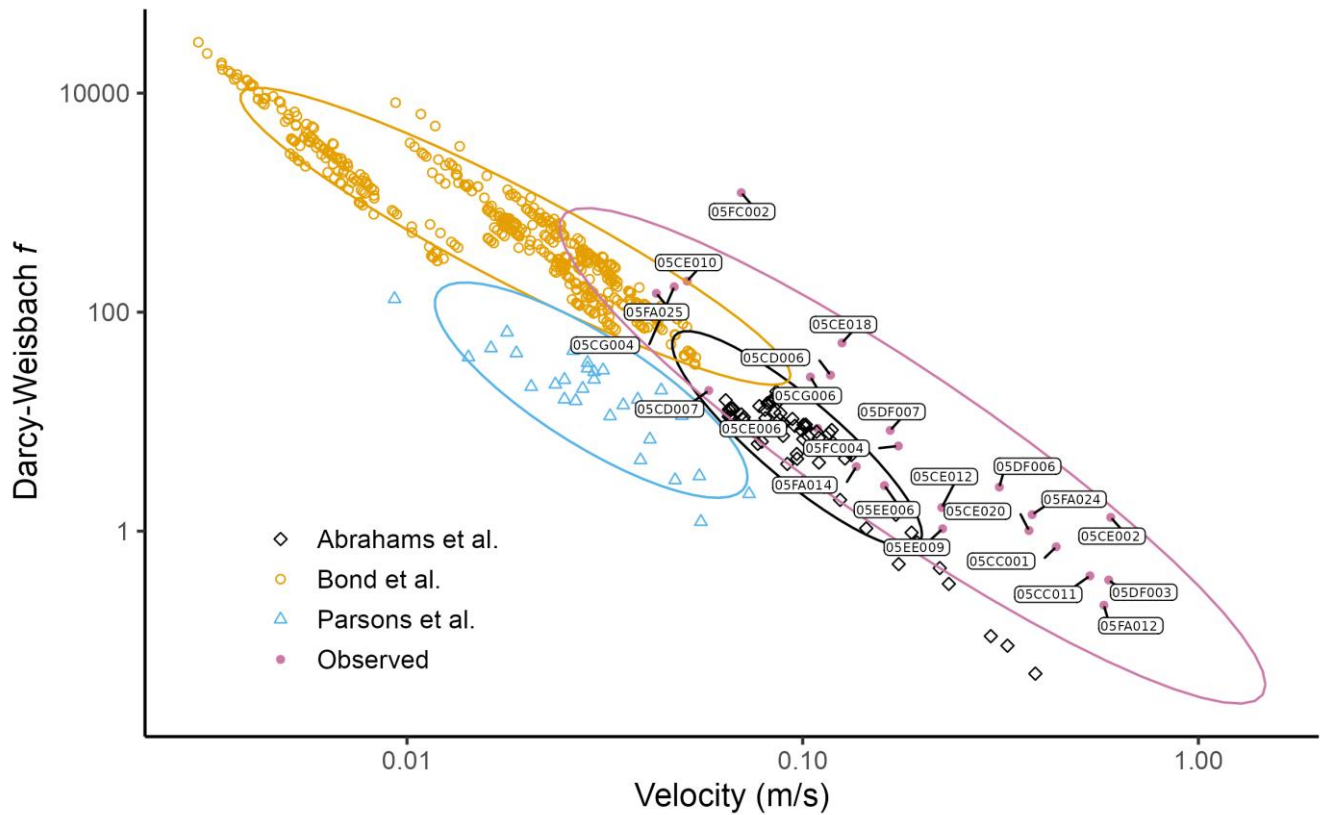
Figure 10: Darcy-Weisbach roughness coefficient (*f*) vs velocity for the study basins ("Observed") and from published values. The ellipses represent multivariate t-distributions fitted to the points. Both axes have logarithmic scales.

5. Discussion

Many of the observed Prairie basin flood wave celerities and velocities are very small. It is apparent that the smallest values of the study celerities and the ratios of basin velocities to stream velocities, and the largest estimated values for Manning's *n* and the Darcy-Weisbach *f*, were obtained from the smallest basins. This indicates that the cause(s) of the exceptionally small basin velocities are related to the presence of overland and/or shallow subsurface flows, as channel flows will dominate at large scales. This finding also agrees with the work of Brannen et al. (2015) and Costa et al. (2020) which were carried out on very small basins. The effects of scale appear to hold true even in the badlands-containing basins (05CE002, 05CE020, and 05FC004) and the montane basin (05CC001), despite the possibility of different predominant flow pathways in these basins from those in the plains.

The channel slopes of the central Alberta basins (Table 1) are gentle and undoubtedly influence basin-scale flow velocities. The equations of Kirpich (1940), Watt and Chow (1985), and Langridge et al. (2020) explicitly include the channel slope. The slopes of the basins studied here are much shallower than those used by Kirpich (1940). The slopes of the study basins

lie within the range of those used by Watt and Chow (1985) to derive their relationship and at least three of the Alberta

445   basins lie within the range of the areas of the basins that they used. However the values of t_{cK} and t_{IW} were much smaller than the observed t_p values. The values of slopes used by Langridge et al. (2020) are unknown but the t_{pL} values were quite similar to the observed t_p values.

Although the equations of Capece et al. (1988) and Sheridan (1994) do not include the channel slope, the basin slopes used for their derivations are similar to the values of the experimental basins. As described above, the t_{IC} values were smaller than

450   the observed t_p values, while the t_{cS} values were quite similar to the observed t_p values.

Therefore, the gentle slopes may not be sufficient on their own to explain the behaviours of the experimental basins. It is believed that there are at least five additional potential causes of the slow responses of the prairie basins: 1) flow paths, 2) climate, 3) depressional storage, 4) roads and culverts, and 5) vegetation. It is quite possible that more than one cause is responsible for the slow responses.

455   Brannen et al. (2015) found evidence of shallow groundwater flows in the hummocky ~1.2 km^2 Brannen sub-basin at SDRB. Using tracers, Ross et al. (2017) found evidence of old water that could rapidly contribute to streamflows in hill slope plots in southern Manitoba. It is unclear whether these results can be extrapolated to the much larger scales of the study basins and to the drier conditions with more frequently unsaturated soils at depth that prevail in western Alberta. Furthermore, the very slow velocities simulated by Costa et al. (2020) did not include sub-surface flows.

460   The effects of low runoff rates in reducing flow velocities were demonstrated by Costa et al. (2020) in simulations of snow melt runoff events. The small annual basin yields in the Prairies described by Bemrose et al. (2009), imply that rainfall events do not often produce large runoff rates, as most of the runoff in the region is due to snow melt. This is particularly likely to be true of the events considered here, which will tend to have low intensities and long durations. Low rates of runoff associated with gentle rainfall will translate to small streamflows. As indicated by Eqs. 8 and 12, the flow velocity increases

465   with the hydraulic radius, which is a function of the depth of flow. Thus, shallow flows resulting from relatively small runoff events will be slow. This may be why the equation of Langridge et al. (2021), which includes representations of the climate and the peak discharge, performed relatively well in this study. Cen et al. (2022) found that unit discharge was the most important factor in determining the transition from laminar to transitional flows, in flume experiments using synthetic vegetation.

470   The ubiquitous depressions within Prairie basins may reduce flow velocities, through at least two mechanisms. The first is by reducing flow rates as runoff water fills the depressions. The small yields of many Prairie basins are caused in part by the reduction of their contributing fractions through the abstraction of runoff by depressions. The reduction in flow rates will contribute to the reduction in runoff velocities. The second mechanism is the reduction of outflow velocities from depressions by widening flow channels. As the land surface slopes upward gradually in all directions, as shown by the

475   scaling equations of Hayashi and van der Kamp (2000), the addition of water to a depression causes a relatively small increase in stage, compared to a channel. Thus, the topography of the depression reduces the head available to drive flows over the outlet sill of the depression.

Koskiaho (2003) found outflow velocities of approximately 0.02 m s^{-1}, when simulating flows within constructed wetlands in Finland. Kadlec (1990) found that surface velocities varied widely at a single wetland site, their histogram varying between 5 and 125 m h^{-1} (0.0014 and 0.035 m s^{-1}).

Depressional storage is unlikely to be the sole cause of the observed long t_p values and the consequent very small magnitudes of the flood wave celerities and velocities. As demonstrated in Table 2, there was no significant correlation between the effective area fractions of the Alberta basins, or their wetland areal percentages, and their observed t_p. The results of Costa et al. (2020), cited in the introduction, were obtained in a basin with relatively little depressional storage. Basin 05CE010 had a very slow celerity/velocity (Fig. 7), and a very large value of n (Fig. 9), for its area, despite having an effective area fraction of 1, as shown in Table 1, suggesting minimal depressional storage.

The Canadian Prairies are divided by a network of roads spaced at intervals of 1.6 or 3.2 km, (i.e. 1 or 2 miles). The roads have deep and broad ditches on either side and are usually provided with culverts to allow water to pass through, but the siting, sizes and conditions of the culverts are rarely optimal. The road bed network is therefore effectively a grid of dams, as has been documented in the United States (Wang et al., 2011), and in Alberta (Duke et al., 2003). It is likely that roads and culverts also contribute to slowing summer runoff in the Alberta study basins in a similar manner as natural depressions.

Kadlec (1990) stated that for wetlands, "Open-channel equations, such as Manning's, should not be used because they apply to situations where bottom drag is controlling. In vegetated wetlands, vegetation drag controls". Vegetation subdivides flow, exerting a shear stress over the submerged depth of stalks. Although the summer rainfall events occur during the growing season, the entire depth of flow is likely to lie within the crop heights, because the flows are shallow, even early in the growing season when the crops (which are primarily annuals) are short.

Horton (1939) described flow velocities in the transition zone between laminar and turbulent flows. For open channels, laminar flows are assumed to occur for Reynolds numbers smaller than 500 (Yen, 2002). Abrahams et al. (1994) found flow velocities between 0.065 and 0.387 m s^{-1} at research plots on semiarid grassland and shrubland hill slopes in Arizona, with Reynolds numbers between 86.5 and 450.2. The smaller velocities on these plots are greater than some of the estimated velocities for the study basins. Bond et al. (2020b) also found many flow measurements lying within the laminar regime, on research plots in northern England. Interestingly, Gilley and Kottwitz (1994) found that wheat stalks had the greatest roughness coefficients of any crop tested (including corn, cotton, sorghum, soybeans and sunflowers) in rectangular flumes, and found Reynolds numbers as small as 500. As wheat is a dominant crop in much of the Canadian prairies, its role in slowing overland flows is expected to be important.

Channels constructed for artificial drainage will behave very differently from the natural swales which exist between depressions. Artificial drainage channels are much narrower for a given depth, and also be straighter and shorter, than natural channels which will result in deeper and faster flows than in natural channels. Therefore, Prairie basins subject to extensive agricultural drainage will, all other factors being equal, experience changes in their response times, introducing yet another degree of nonstationarity which must be modelled. White et al. (2003) found that channel drainage of basins in Illinois decreased their times to peak. Artificial drainage may also increase water velocities by increasing flowrates, through the

elimination of depressional storage. Thus, models calibrated against historical streamflows will be very vulnerable to errors when simulating the effects of drainage in Prairie basins.

6. Conclusions

515   The observed t_p values estimated from the streamflow hydrometric records were generally much greater than estimated by 4 of the 6 available empirical equations. There were no apparent relationships between the study t_p values and any of the basins' characteristics. The only relationship that possibly described the runoff velocities was a weak power-law fit with the basin gross areas.

The slow observed responses and estimated flow velocities of the basins have important implications for Canadian Prairie 520   hydrology, particularly for modelling stream flow responses to rainfall using hydrological routing. Many engineering design calculations, such as the Rational Method and dimensionless hydrographs, such as the SCS Unit Hydrograph, are based on empirical response times, such as t_c and t_p. As four of the six empirical equations, grossly underestimate the hydrological response times of the study basins, these methods are likely to cause large errors in design flows. The equations of Sheridan (1994) and Langridge et al. (2021) provide better estimates of the basin response times, although they show considerable 525   scatter.

Development of routing methods suitable for Prairie basins will require understanding of flow velocities at many scales within basins. Distributed hydrological models are being used in the Canadian Prairies, with grid scales varying from 125 km^2 (Hossain, 2017) to as small as 1 km^2 (Mengistu and Spence, 2016) and presume turbulent flow in their hydrological routing methods. The demonstrated relationships between the basin velocity and area indicates that the size of the region 530   being modelled must be taken into account when developing routing methods for such models. Calibrated roughness parameters cannot be separated from their scales and the assumption of turbulence is highly uncertain. As many modellers restrict calibrated values to be within the range of published values, the use of Manning's equation, which may require unreasonable values of *n* to work, will induce errors in other calibrated parameters of a model. The Darcy-Weisbach equation, which can simulate all flow regimes, appears to be better suited to Canadian Prairie basins. The basin-scale 535   velocities were much smaller than stream velocities at the gauges, also indicating that gauged data do not well represent basin-scale behaviours.

This study is a first step on the path toward understanding and modelling flow velocities in the Canadian Prairies. Further research will be required to determine the small-scale velocities of flows, and to find ways of incorporating their spatial and temporal variabilities in basin-scale hydrological models of this region. Further modelling and field work studies, perhaps 540   involving the use of tracers, are needed to gain a better understanding of why basin-scale responses and velocities in the region are as slow as are found here.

Code and data availability. All data, **R** code, and calculation results used in this research are published online at https://zenodo.org/record/7915938.

Author contribution. KRS and PHW conceived the study and led the analyses. CS supplied experimental data. All authors contributed to the writing.

Competing interests. The contact author has declared that none of the authors has any competing interests.

Acknowledgments The authors acknowledge funding support from Global Water Futures and Environment and Climate Change Canada.

We would also like to acknowledge the assistance of officials from the Water Survey of Canada of Environment and Climate Change Canada in providing us access to hydrometric basin shape files, hourly streamflows and manual gauging data. This research could not have been undertaken without their support.

References

Abrahams, A. D., Parsons, A. J., and Wainwright, J.: Resistance to overland flow on semiarid grassland and shrubland hillslopes, Walnut Gulch, southern Arizona, Journal of Hydrology, 156, 431–446, https://doi.org/10.1016/0022-1694(94)90088-4, 1994.

Agriculture and Agri-food Canada: Land Cover for Agricultural Regions of Canada, circa 2000 - Open Government Portal, 2009.

Alberta Agriculture and Forestry, Government of Alberta: Areal Extent of Wetlands, Areal Extent of Wetlands, 2016.

Anderson, E., Chlumsky, R., McCaffrey, D., Trubilowicz, J., Shook, K. R., and Whitfield, P. H.: R-functions for Canadian hydrologists: A Canada-wide collaboration, Canadian Water Resources Journal / Revue canadienne des ressources hydriques, 44, 108–112, https://doi.org/10.1080/07011784.2018.1492884, 2019.

Bemrose, R., Kemp, L., Henry, and Soulard, F.: Water Yield for Canada as a Thirty-year Average (1971 to 2000): Concepts, Methodology and Initial Results, Statistics Canada Research and development section, Ottawa, Ontario, Canada, 2009.

Beven, K. J.: A history of the concept of time of concentration, Hydrology and Earth System Sciences, 24, 2655–2670, https://doi.org/10.5194/hess-24-2655-2020, 2020.

Bjerklie, D. M.: Estimating the bankfull velocity and discharge for rivers using remotely sensed river morphology information, Journal of Hydrology, 341, 144–155, https://doi.org/10.1016/j.jhydrol.2007.04.011, 2007.

Bond, S., Kirkby, M. J., Johnston, J., Crowle, A., and Holden, J.: Seasonal vegetation and management influence overland flow velocity and roughness in upland grasslands, Hydrological Processes, 34, 3777–3791, https://doi.org/10.1002/hyp.13842, 2020a.

Bond, S., Kirkby, M. J., Johnston, J., Crowle, A., and Holden, J.: Seasonal vegetation and management influence overland flow velocity in upland grasslands - dataset, https://doi.org/10.5518/794, 2020b.

Brannen, R.: Controls on connectivity and streamflow generation in a Canadian Prairie landscape, Master's thesis, University of Saskatchewan, Saskatoon, Saskatchewan, Canada, 2015.

575 Brannen, R., Spence, C., and Ireson, A.: Influence of shallow groundwater-surface water interactions on the hydrological connectivity and water budget of a wetland complex, Hydrological Processes, 29, 3862–3877, https://doi.org/10.1002/hyp.10563, 2015.

Capece, J. C., Campbell, K. L., and Baldwin, L. B.: Estimating Runoff Peak Rates from Flat, High-Water-Table Watersheds, Transactions of the ASAE, 31, 0074–0081, https://doi.org/10.13031/2013.30668, 1988.

580 Cen, Y., Zhang, K., Peng, Y., Rubinato, M., Liu, J., and Ling, P.: Experimental study on the effect of simulated grass and stem coverage on resistance coefficient of overland flow, Hydrological Processes, 36, e14705, https://doi.org/10.1002/hyp.14705, 2022.

Christiansen, E. A.: The Wisconsinan deglaciation of southern Saskatchewan and adjacent areas, Canadian Journal of Earth Sciences, 16, 913–938, 1979.

585 Costa, D., Shook, K., Spence, C., Elliott, J., Baulch, H., Wilson, H., and Pomeroy, J. W.: Predicting Variable Contributing Areas, Hydrological Connectivity, and Solute Transport Pathways for a Canadian Prairie Basin, Water Resources Research, 56, e2020WR027984, https://doi.org/10.1029/2020WR027984, 2020.

de Boer, D. H. and Campbell, I. A.: Spatial scale dependence of sediment dynamics in a semi-arid badland drainage basin, CATENA, 16, 277–290, https://doi.org/10.1016/0341-8162(89)90014-3, 1989.

590 Duke, G. D., Kienzle, S. W., Johnson, D. L., and Byrne, J. M.: Improving overland flow routing by incorporating ancillary road data into digital elevation models, Journal of Spatial Hydrology, 3, 2003.

Dumanski, S., Pomeroy, J. W., and Westbrook, C. J.: Hydrological regime changes in a Canadian Prairie basin, Hydrol. Process., 29, 3893–3904, https://doi.org/10.1002/hyp.10567, 2015.

Ellis, W. H. and Gray, D. M.: Interrelationships Between the Peak Instantaneous and Average Daily Discharges of Small

595 Prairie Streams, Canadian Agricultural Engineering, 2–5, 1966.

Farr, T. G., Rosen, P. A., Caro, E., Crippen, R., Duren, R., Hensley, S., Kobrick, M., Paller, M., Rodriguez, E., Roth, L., Seal, D., Shaffer, S., Shimada, J., Umland, J., Werner, M., Oskin, M., Burbank, D., and Alsdorf, D.: The Shuttle Radar Topography Mission, Reviews of Geophysics, 45, https://doi.org/10.1029/2005RG000183, 2007.

Ferguson, R.: Time to abandon the Manning equation?, Earth Surface Processes and Landforms, 35, 1873–1876,

600 https://doi.org/10.1002/esp.2091, 2010.

Gericke, O. J. and Smithers, J. C.: Review of methods used to estimate catchment response time for the purpose of peak discharge estimation, Hydrological Sciences Journal, 59, 1935–1971, https://doi.org/10.1080/02626667.2013.866712, 2014.

Gilley, J. E. and Kottwitz, E. R.: Darcy-Weisbach Roughness Coefficients for Selected Crops, Transactions of the ASAE, 37, 467–471, https://doi.org/10.13031/2013.28098, 1994.

605 Gilley, J. E., Flanagan, D. C., Kottwitz, E. R., and Weltz, M. A.: Darcy-Weisbach roughness coefficients for overland flow, in: Overland flow, edited by A. Parsons and A. Abrahams, 24–47, 1992.

Godwin, R. B. and Martin, F. R. J.: Calculation of gross and effective drainage areas for the Prairie Provinces, in: Proceedings of Canadian Hydrology Symposium, 219–223, 1975.

Government of Alberta: Wetland Regulatory Requirements Guide, Water Policy Branch, 2015.

610 Gray, D. M.: Interrelationships of Watershed Characteristics, Journal of Geophysical Research, 66, 1215–1223, https://doi.org/10.1029/JZ066i004p01215, 1961.

Grimaldi, S., Petroselli, A., Tauro, F., and Porfiri, M.: Time of concentration: A paradox in modern hydrology, Hydrological Sciences Journal, 57, 217–228, https://doi.org/10.1080/02626667.2011.644244, 2012.

Hayashi, M. and van der Kamp, G.: Simple equations to represent the volume-area-depth relations of shallow wetlands in
615 small topographic depressions, Journal of Hydrology, 237, 74–85, https://doi.org/10.1016/S0022-1694(00)00300-0, 2000.

Hijmans, R. J.: Raster: Geographic data analysis and modeling, 2020.

Holtan, H. N. and Overton, D. E.: Analyses and application of simple hydrographs, Journal of Hydrology, 1, 250–264, https://doi.org/10.1016/0022-1694(63)90005-2, 1963.

Horton, R. E.: The Interpretation and Application of Runoff Plat Experiments with Reference to Soil Erosion Problems, Soil
620 Science Society of America Journal, 3, 340, https://doi.org/10.2136/sssaj1939.036159950003000C0066x, 1939.

Hossain, K. 1986.-.: Towards a Systems Modelling Approach for a Large-Scale Canadian Prairie Watershed, Master's thesis, University of Saskatchewan, Saskatoon, Saskatchewan, Canada, 2017.

James, W. P., Winsor, P. W., and Williams, J. R.: Synthetic Unit Hydrograph, Journal of Water Resources Planning and Management, 113, 70–81, 1987.

625 Kadlec, R. H.: Overland Flow in Wetlands: Vegetation Resistance, Journal of Hydraulic Engineering, 116, 691–706, https://doi.org/10.1061/(ASCE)0733-9429(1990)116:5(691), 1990.

Kirpich, Z. P.: Time of concentration of small agricultural watersheds, Civil engineering, 10, 362, 1940.

Koskiaho, J.: Flow velocity retardation and sediment retention in two constructed wetland-ponds, Ecological Engineering, 19, 325–337, https://doi.org/10.1016/S0925-8574(02)00119-2, 2003.

630 Langridge, M., Gharabaghi, B., McBean, E., Bonakdari, H., and Walton, R.: Understanding the dynamic nature of Time-to-Peak in UK streams, Journal of Hydrology, 583, 124630, https://doi.org/10.1016/j.jhydrol.2020.124630, 2020.

Langridge, M., McBean, E., Bonakdari, H., and Gharabaghi, B.: A dynamic prediction model for time-to-peak, Hydrological Processes, 35, e14032, https://doi.org/10.1002/hyp.14032, 2021.

LaZerte, S. and Albers, S.: Weathercan: Download and format weather data from Environment and Climate Change Canada,
635 Journal of Open Source Software, 3, 571, https://doi.org/10.21105/joss.00571, 2018.

Leibowitz, S. G. and Vining, K. C.: Temporal connectivity in a prairie pothole complex, Wetlands, 23, 13–25, https://doi.org/10.1672/0277-5212(2003)023[0013:TCIAPP]2.0.CO;2, 2003.

Leroux, N. R. and Pomeroy, J. W.: Modelling capillary hysteresis effects on preferential flow through melting and cold layered snowpacks, Advances in Water Resources, 107, 250–264, https://doi.org/10.1016/j.advwatres.2017.06.024, 2017.

640 Lindsay, J. B.: Whitebox GAT: A case study in geomorphometric analysis, Computers & Geosciences, 95, 75–84, https://doi.org/10.1016/j.cageo.2016.07.003, 2016.

McCuen, R. H.: Uncertainty Analyses of Watershed Time Parameters, Journal of Hydrologic Engineering, 14, 490–498, https://doi.org/10.1061/(ASCE)HE.1943-5584.0000011, 2009.

McDonnell, J. J. and Beven, K.: Debates - The future of hydrological sciences: A (common) path forward? A call to action aimed at understanding velocities, celerities and residence time distributions of the headwater hydrograph, Water Resources Research, 50, 5342–5350, https://doi.org/10.1002/2013WR015141, 2014.

McDonnell, J. J., Spence, C., Karran, D. J., Van Meerveld, H. J., and Harman, C. J.: Fill-and-spill: A process description of runoff generation at the scale of the beholder, Water Resources Research, 57, e2020WR027514, 2021.

Mengistu, S. G. and Spence, C.: Testing the ability of a semidistributed hydrological model to simulate contributing area, Water Resources Research, 52, 4399–4415, https://doi.org/10.1002/2016WR018760, 2016.

Natural Resources Canada: National Hydro Network, Canada, Level 1 Linear Referencing System (LRS) Data Catalogue Edition 1.0, Natural Resources Canada Geomatics Canada Centre for Topographic Information, 2004.

Pebesma, E. and Bivand, R. S.: S classes and methods for spatial data: The sp package, R news, 5, 9–13, 2005.

Pebesma, E. J.: Multivariable geostatistics in S: The gstat package, Computers & Geosciences, 30, 683–691, https://doi.org/10.1016/j.cageo.2004.03.012, 2004.

Pennock, D., Bedard-Haughn, A., and Viaud, V.: Chernozemic soils of Canada: Genesis, distribution, and classification, Can. J. Soil. Sci., 91, 719–747, https://doi.org/10.4141/cjss10022, 2011.

Pomeroy, J. W., Gray, D. M., and Landine, P. G.: The Prairie Blowing Snow Model: Characteristics, validation, operation, Journal of Hydrology, 144, 165–192, https://doi.org/10.1016/0022-1694(93)90171-5, 1993.

Pomeroy, J. W., Gray, D. M., Shook, K. R., Toth, B., Essery, R. L. H., Pietroniro, A., and Hedstrom, N.: An evaluation of snow accumulation and ablation processes for land surface modelling, Hydrological Processes, 12, 2339–2367, https://doi.org/10.1002/(SICI)1099-1085(199812)12:15<2339::AID-HYP800>3.0.CO;2-L, 1998.

QGIS Development Team: QGIS Geographic Information System, Open Source Geospatial Foundation, 2009.

R Core Team: R: A language and environment for statistical computing, R Foundation for Statistical Computing, Vienna, Austria, 2013.

Rosgen, D. L.: A classification of natural rivers, CATENA, 22, 169–199, https://doi.org/10.1016/0341-8162(94)90001-9, 1994.

Ross, C. A., Ali, G., Bansah, S., and Laing, J. R.: Evaluating the Relative Importance of Shallow Subsurface Flow in a Prairie Landscape, Vadose Zone Journal, 16, 1–20, https://doi.org/10.2136/vzj2016.10.0096, 2017.

Schneider, V. and Arcement, G.: Guide for selecting manning's roughness coefficients for natural channels and flood plains, Available from the US Geological Survey, Books and Open-File Reports Section, Box 25425, Federal Center, Denver, CO 80225-0425. Water-Supply Paper 2339, 1989. 38 p, 22 fig, 4 tab, 23 ref., 1989.

Schroers, S., Eiff, O., Kleidon, A., Scherer, U., Wienhöfer, J., and Zehe, E.: Morphological controls on surface runoff: An interpretation of steady-state energy patterns, maximum power states and dissipation regimes within a thermodynamic framework, Hydrology and Earth System Sciences, 26, 3125–3150, https://doi.org/10.5194/hess-26-3125-2022, 2022.

Sharratt, B., Benoit, G., Daniel, J., and Staricka, J.: Snow cover, frost depth, and soil water across a prairie pothole landscape, Soil science, 164, 483–492, 1999.

Shaw, D. A., van der Kamp, G., Conly, F. M., Pietroniro, A., and Martz, L.: The Fill-Spill Hydrology of Prairie Wetland Complexes during Drought and Deluge, Hydrological Processes, 26, 3147–3156, https://doi.org/10.1002/hyp.8390, 2012.

680   Sheridan, J. M.: Hydrograph Time Parameters for Flatland Watersheds, Transactions of the ASAE, 37, 103–113, https://doi.org/10.13031/2013.28059, 1994.

Shook, K. and Gray, D. M.: Synthesizing shallow seasonal snow covers, Water Resources Research, 33, 419, https://doi.org/10.1029/96WR03532, 1997.

Shook, K. and Pomeroy, J.: Changes in the hydrological character of rainfall on the Canadian prairies, Hydrological

685   Processes, 26, 1752–1766, https://doi.org/10.1002/hyp.9383, 2012.

Shook, K., Pomeroy, J. W., Spence, C., and Boychuk, L.: Storage dynamics simulations in prairie wetland hydrology models: Evaluation and parameterization, Hydrological Processes, 27, 1875–1889, https://doi.org/10.1002/hyp.9867, 2013.

Siemonsma, D.: The Shuttle Radar Topography Mission (SRTM) Collection User Guide, 17, 2015.

Spence, C. and Woo, M. K.: Hydrology of subarctic Canadian shield: Soil-filled valleys, Journal of Hydrology, 279, 151–

690   166, https://doi.org/10.1016/S0022-1694(03)00175-6, 2003.

Stichling, W. and Blackwell, S. R.: Drainage Area as a Hydrologic Factor on the Glaciated Canadian Prairies, in: IUGG Proceedings, Volume 111, 365–376, 1957.

Szeto, K., Gysbers, P., Brimelow, J., and Stewart, R.: The 2014 extreme flood on the southeastern Canadian prairies, Bulletin of the American Meteorological Society, 96, S20–S24, 2015.

695   Wang, X., Liu, T., Yang, D., Qu, Z., Clary, C. R., and Wunneburger, C.: Simulating Hydrologic Effects of Raised Roads within a Low-Relief Watershed, Journal of Hydrologic Engineering, 16, 585–597, https://doi.org/10.1061/(ASCE)HE.1943-5584, 2011.

Watt, W. E. and Chow, K. C. A.: A general expression for basin lag time, Can. J. Civ. Eng., 12, 294–300, https://doi.org/10.1139/l85-031, 1985.

700   Weltz, M. A., Arslan, A. B., and Lane, L. J.: Hydraulic Roughness Coefficients for Native Rangelands, Journal of Irrigation and Drainage Engineering, 118, 776–790, https://doi.org/10.1061/(ASCE)0733-9437(1992)118:5(776), 1992.

White, A. B., Kumar, P., Saco, P. M., Rhoads, B. L., and Yen, B. C.: Changes in Hydrologic Response Due to Stream Network Extension Via Land Drainage Activities, Journal of the American Water Resources Association, 39, 1547–1560, https://doi.org/10.1111/j.1752-1688.2003.tb04438.x, 2003.

705   Willis, W. O., Carlson, C. W., Alessi, J., and Haas, H. J.: Depth of Freezing and Spring Run-Off as Related to Fall Soil-Moisture Level, Can. J. Soil. Sci., 41, 115–123, https://doi.org/10.4141/cjss61-014, 1961.

Wong, T. S. and Zhou, M. C.: Kinematic Wave Parameters for Trapezoidal and Rectangular Channels, J. Hydrol. Eng., 11, 173–183, https://doi.org/10.1061/(ASCE)1084-0699(2006)11:2(173), 2006.

Woo, M.-K. and Sauriol, J.: Channel Development in Snow-Filled Valleys, Resolute, N. W. T., Canada, Geografiska
710   Annaler. Series A, Physical Geography, 62, 37–56, https://doi.org/10.2307/520451, 1980.

Yen, B. C.: Open Channel Flow Resistance, Journal of Hydraulic Engineering, 128, 20–39,
https://doi.org/10.1061/(ASCE)0733-9429(2002)128:1(20), 2002.